A PROPOSAL OF NEW METHOD FOR ESTIMATING DEPTH OF CURIE SURFACE (*)

Paulo C. Soares - FUNPAR/UFPR, Francisco J. F. Ferreira – UFPR, Alberto P. Fiori – UFPR Luis Gustavo Castro – UFPR, Silvana B. Riffel – Brisbane University.
(*)A contribution from Projeto Falhas.

This paper was prepared for presentation during the 11th International Congress of the Brazilian Geophysical Society held in Salvador, Brazil, August 24-28, 2009.

Abstract

The power density spectrum of magnetic anomaly based on radial average is a procedure commonly used to estimate the depth of the Curie surface. Many applications are found in the literature, for different geological contexts. Despite this, some methodological and operational difficulties are present: (1) radial average, assuming a priori that the medium is isotropic and that there is a single point to start the Fourier transform; (2) difficulty and ambiguity in determining the segment containing the points of similar inclination: (3) the need for manual procedure on examination of the spectrum. An alternative method is investigated and presented in this work. The first is the decomposition of oscillatory series by analysis of variance instead of Fourier analysis; the second is to use variogram to determine the wavelengths and the third is the use covariance spectrum as function of wavelength as a power spectrum. The method was tested on an area east of the Paraná basin, where determinations of Curie depth and heat flux from temperatures in oil wells are found of in the literature.

Resumo

Um procedimento comumente utilizado para estimar a profundidade da superfície Curie é espectro de densidade de potência de anomalia magnética com base na média radial. Muitas aplicações são encontradas na literatura, para diferentes contextos geológicos. Apesar disso, algumas dificuldades metodológicas e operacionais estão presentes: (1) média radial, assumindo a priori que o meio é isotrópica e que existe um ponto para iniciar a transformada de Fourier; (2) a dificuldade e ambiguidade na determinação do segmento que contém os pontos de inclinação similar no espectro; (3) a necessidade de procedimento manual no exame do espectro. Um método alternativo é investigado e apresentado neste trabalho. A primeira diferença é a decomposição da série oscilatória por análise de variância em vez de análise de Fourier; a segunda é o uso do variogram para determinar os comprimentos de onda e o terceiro é o espectro de covariância de uso em função do comprimento de onda como um espectro de potência. O método foi testado em uma área a leste da bacia do Paraná, onde determinações de fluxo de calor e profundidade de Curie de temperaturas em poços de petróleo são encontradas de na literatura.

Introduction

In many regions, due to the formation of continental crust, by accreting or collision of different terrains, strong geophysics anisotropy is a feature of the basement. This is recorded in magnetic signal directional variability, making it inapplicable to classical use power density spectrum obtained by the average radial magnetic anomaly (Oukbo et al., 1985). In addition, in the current procedure, the establishment of the line segment in the first part of the power spectrum is difficult and somewhat ambiguous, because often the segment is a broken line. Additionally instead of wave number, it is used the wavelength, because being very long waves, over one hundred kilometers, scale problems emerge in log of wave number: on a scale from 1 to 0.001, the work values relevant to determination of surface Curie are between 0.02 and 0.01/km.

Thus, this proposition investigates the potential of variogram and covariogram as magnetic signal analyzer and estimator of power spectrum.

The test area is a geological site in Parana Basin, South Brazil, which has long history of tectonic activity. The major structure is the Lancinha fault zone (Cubatão-Paraíba Lineament) extending from Campo Largo (Paraná State) to Caçador (Santa Catarina State).

Background

The disappearance in depth of the sources of magnetic anomalies can be attributed to an isotherm higher than the Curie temperature of magnetite (around 575 ^{o}C). The surface formed by points at different depths (Curie depth, Pc) where this critical temperature occurs is called the Curie surface (CS).

In continental areas, for Tc=575 ^{o}C, $Pc=k_T.\ 550/Q$, k_T ~ 2.4 w/(m.^{o}C, regional Q flow between 50 and 60 mw/m2, the expected depth of the Curie isotherm (PSC), would be between 22 and 24 km. As heat flow measurements are very sparse, one way to establish zones of thermal anomalies is the mapping of depth Curie, the relation

between the deep of magnetic source and size of the anomaly generated.
The relationship between magnetic field power measured in a horizontal plane with the geometry and properties of the source of the anomaly has been represented by the expression of Naidu (1968). Taken an isotropic or one-directional field, depth of source small compared to horizontal extension of anomaly and randomly varying magnetization within the body, simplifications are possible (Blakely, 1995; Tanaka et al. 1999; Maden, 2009).
Considering the set of spatial variables as constants for the same source and domain, the power *F(s)* of the signal with wave number *s* is simplified as exponential function of *zt, zb* and *h*, representing the depth from the top, bottom and thickness of the body respectively. Relations with body geometry, with its spatial position and distance from the observer, with their position in relation to strike and variation of magnetic field strength, with the presence of anisotropy of the body, and a superposition of sources impose algebraic difficulties to obtain the value of *F*. The procedure of radial average power, widely used abroad (Okubo et al. 1985) and in Brazil (Blum & Pires 1995; Ferreira et al 1996; Soares et al. 1996) shows high imprecision in areas with large anisotropy. Algebraic solutions obtained directly from the exponential relationship of Naidu (1968) between geometry and signal power was developed and used by Maus et al. (1999) and Aydin and Oksum (2010). The last contribution results are closer to the values entered in simulations and comparatively better than those obtained by spectral analysis. However, both offer distortions and bias as shown by simulation results represented in figure 1.

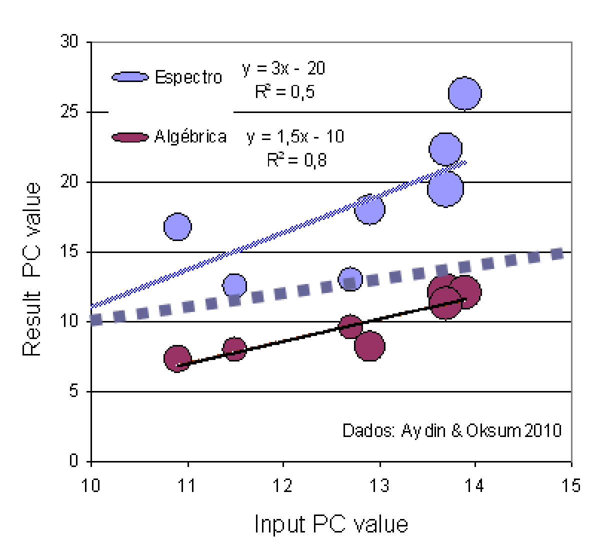

Figure 1 Relationship between inputs and results values of depth for top and bottom of prismatic sources of total magnetic field anomalies in synthetic 2D models, with parameters similar to reality.

The algebraic solution is more stable than the spectral solution. On average, the results of the spectral analysis overestimate solution by 50% of the input values, while the algebraic underestimate solution at 25%.
These are the reason to search for an alternative method.

Analysis of magnetic signal

The determination of wavelengths and amplitudes components of a signal f (x, y) can be done by the Fourier transform of the signal. Alternatively, it can be used statistical methods such as periodogram and the correlogram, once self-variance is at maximum when the lag is equal to half wavelength and minimum when equal. The power of a signal is given by the average square of oscillation around zero. For sinusoidal signals, it is equal to squared amplitude, equal to covariance.

With discrete variables. The Fourier transform, as a function of wavelength, is given by the mean value of signal. The solution to the complex number contains the real (R) and imaginary (I) parts, given by average of products of the signal f (k) by the cosine or sine, respectively, of the wave height in fraction k/N, or k. Δx/λ. The value of the module of the amplitude of each wave is given by the root of the sum of the squares of the two parties and the phase by the ratio between I and R.
The samples used in the calculation of each term must keep the distance k. Δx among themselves (more allowable tolerance). The operating procedure in 2D (X, Y) is made from a source, a central point, around which different circumferences radii k. Δx are computed for the average value of *F*.

The same space series formed by data sampling of function f (x) along the X has mean (m) and variance (V).

If we compare the series with its replica, displacing the replica along X by a step kx = k.Δx, and making the two series to translate in X, we can estimate the auto-covariance of f (x) with f (x + kx). This value gives an estimate of the autocorrelation and variogram function of kx.
When signals f (x) and f (x + kx) are homologues in the sinusoidal waves (with amplitude A and wavelength λ) the product is positive and reaches maximum (A^2) value for kx=λ. When opposites (λ/2) it takes the minimum value.
On the other hand, the Variogram is a complementary function of Covariance around Variance, for stationary series, when f (x) and f (x + k) have the same average and variance.
When signals f (x) and f (x + kx) are opposite (kx = λ/2), maximum value ($4A^2$) and when counterparts (k x = λ) quadratic difference is minimal.
Both variograma and covariogram functions replicate the average signal and can be converted into averaged f(x).
The average values of the maximum total height of covariogram and the variogram are equal and correspond to the square of the amplitude of oscillation maximum. For a wave length λ in step k = λ/2, the value of γ (quadratic difference of height) reaches the maximum, being equal

$$\gamma_{(k=\lambda/2)} = \frac{2}{k} . \sum_{i=1}^{k} (a_i^{\ 2}) \qquad (1)$$

The term i of larger value occurs for λ/4, when height a_i equal amplitude A. The mean-squared amplitude of the wave of λk = kx is given by $\gamma(k_x/2)$ of the respective step:

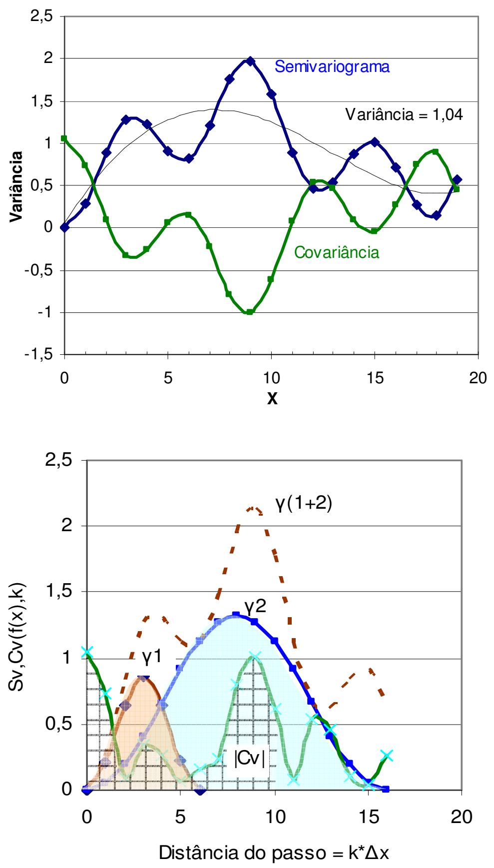

Figure 2 (A) Representation of covariance and variogram of a signal f (x) composed of two oscillatory waves with λ1 = 6 and λ2 = 16 (variance = 1.04). (B) -Cumulative nature of the functions of variability. The area under γ (1 + 2) comprises of γ1 and γ2, signs of signs f (λ1 and λ2). The area under |Cv | from 0 up to 16, corresponds to energy and (λ = 16). For various wavelengths λi = x = k. Δx, Cv values represent the square of function f (x) and the area under Cv represents the energy contained in the spectrum from 0 until k. Δx.

$$A_{(\lambda=kx)}{}^{2} = \gamma_{kx/2} = V - Cv \qquad (2)$$

The values of wavelengths components are given respectively by the double values of x extension of the steps with peaks values of γ(x).

This property allows determining the magnitude of the wave with half the wavelength, using the derivative of the variogram function. In the example (figure 2), kx = 3, λ1 = 6 and A1 = 1.13; k=9, kx=8, λ2 =16 and A2 = 1, 4.

Power spectrum of the signal

The power of a signal is the average energy per unit of measurement of wavelength, corresponding to the value of the covariance of step equal to the wavelength

$$P_{(i,\lambda=kx)} = | Cv_{(kx)} | . \qquad (3)$$

Given by variogram, the power of the wave of wavelength i_f, is:

$$P_{(i,\lambda=kx)} = \gamma_{(kx=\lambda/2)} / 2 \qquad (4)$$

For a signal with recurrence of two or more sine waves, the variogram presents a composition with the sum of the amplitudes of the signals. In this case, it becomes necessary to decompose for different waves. As each wave generates a maximum increment of variance in half the wavelength, it becomes relatively easy to identify this position, with a maximum inclination, followed by a reversal or leveling (figure 2). These positive points of inflection (convex upwards) are identified by the first derivative peaks and zero values of the second derivative of γ(x) (figure 2 and 3).

Amplitude determination: Regularization of variogram

Variogram and covariogram reproduce the mean root square signal. Therefore, the bigger waves contain the variability of wavelengths. To remove this cumulative effect and to isolate the effect of desired longer wavelengths only, a filter was used; it is formed by moving average in a window with a half of lag length. In this case only oscillations of λ equal to or greater than are contributing to the composition of covariance (figure 4).

At this point, some remarks are extracted:

1. Each depression, terrace or ramp smoothing in variogram corresponds to decreasing of wave energy, from λ/2 until λ, with the point of reversal in negative or hollow break;

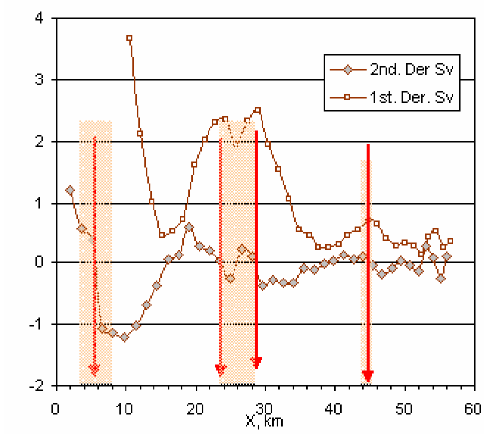

Figure 3 Example of the application o first and second derivative of variogram to identify mean wavelength of wave clusters: γ'>0 and γ"=0 (actual case, cel 10)

2. Each ascending ramp or crest corresponds to increasing energy of the first half of the wavelength λ/2 distinct until,
3. Positive break point or maximum convexity corresponds to half the length of a new distinct wave, i.e., when swallow and swell participate in pair group.
4. The value of γ at this positive break point or peak, corresponds to twice the power of the wave (γ = a2; P = a2/2) and is positioned at half wavelength ($\lambda=2.k_x$ and $\gamma_n=\gamma_{(k=\lambda n/2)}$).

Application of DFT in covariogram and variogram

Application of DFT to correlogram or covariogram (figure 4) may also facilitate the determination of wave components and their powers. The relationship is known as the Wiener-Khinchin Theorem, with easy verification, and allows estimating the spectral density of the signal f (x) by the value of the function of autocovariance C (k).
In the figure 4, the average variograma function (GAMA, moving average) shows notable variance increments for step 12 and 35 km, indicating oscillations with λ 24 and 70 km; secondly, an increment in 22 km. The oscillations of 24 and 44 km are well defined in Fourier transform of correlation (DFT_cor). The power values given by covariance (COV): wave 1 (λ = 24 km) is 82 nT2 and wave 2 (λ = 44 km) is 74 nT2. As the variogram identifies a half wavelength, the longest wavelength is identified (3) with 70 km and covariance Cv = 80 nT2. .
The peaks of DFT appear smoothed by virtue of the fact that the waves of each group do not have the same wavelength, but an approximation around the average.

Value of power for a specific wave signal

Identifying the wavelength in the moving average variogram and the average wave power by covariance value provides the two parameters needed to represent each wave component of the signal.
Therefore, it is possible to select the longer wavelength and its power.

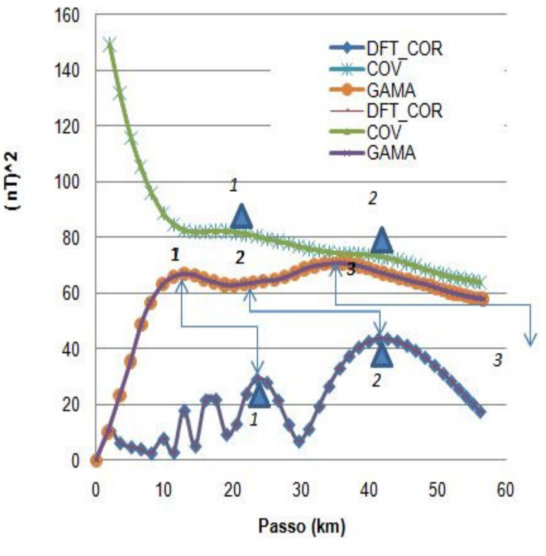

Figure 4 –Moving average Variogram (Gama), Covariance (Cov) for actual data in case FLC cel 10: numbers indicate wave clusters (1, 2, 3) defined in the variogram, covariogram and by the FFT of Covariance. The coordinate values of the points are the power values of the clusters.

Estimation of Depth Curie

For depth *h* of top and thickness *d* the general expression of Naidu (1968) may be written:

$$F_{(s)} = A[e^{-4\pi sd}(1-2e^{-h}) + e^{-4\pi s(d+h)}] \qquad (5)$$

In this case, for values of h/d > 5 and w > 0.6 (λ < 10), the first term can be dismissive, it allows calculating *zb* from *F(λ) or Cv(λ). A* is the *F(s)* value for minimum *s(d+h)*, which is the independent Variance.

$$z_b = -\frac{1}{4\pi}.\lambda.\ln(\frac{F_{(s)}}{A}) \qquad (6)$$

Application in the Paraná basin

The application of the methodology was done in an area of southeast Paraná basin, states of Paraná and Santa Catarina, South Brazil. It includes sedimentary outcrop belt of Ordovician to Jurassic rocks, part of Cretaceous basalt cover and Precambrian basement (figure 5). Many lineaments have been drawn by various authors and through various methods, including geomorphic, spectrometric, magnetic and gravimetric (Soares et al. 2007). The extension of mega faults Lancinha (FL) and Itapirapuã, both active throughout the Phanerozoic to Recent, cross the area, attested by the alignment of the Iguaçu River. Curie Surface is expected to be shallow along these fault zones.

Heat flow estimates are of great utility to validate the results. The results in the test area, although very sparse, obtained for temperature profile from oil wells fluctuate between 35 and 80 mw/m2, giving an idea of the expected PSC for the area.

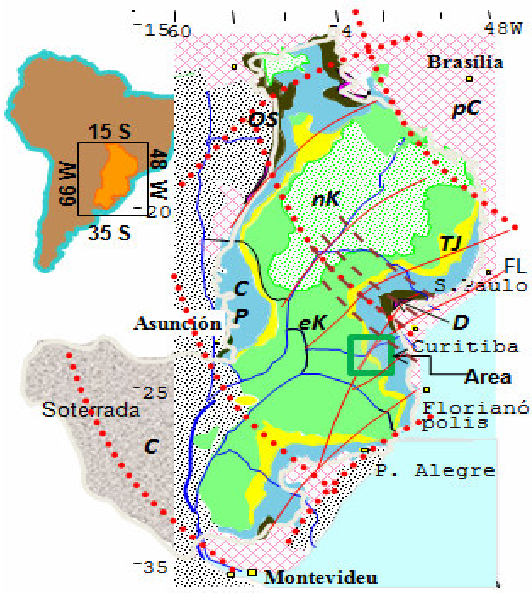

Figure 5 - Location of the area (green square) in the Paraná basin, with outcropping rocks of different type and ages (Precambrian to Cretaceous), current arcs (dotted), mega faults (lines) and diabase dykes (dashed).

Although the number of points of measured temperatures and heat flow estimates are small and dispersed, which does not allows to define zones, as narrow as 10-20 km,

possibly associated with recent faulting, they are good guiders to the results from magnetic data.
For this reason, the estimated values were used to contour using fault boundaries (figure 6).
There are noteworthy anomalies and breaks associated to some blocks and faults.

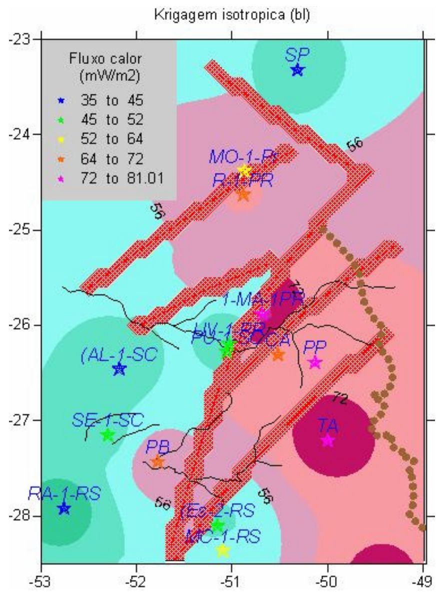

Figure 6 - Heat flow (mW/m2) map (estimated values by Hurter and Pollack 1996; Hamza and Munhoz 1996 Rocha 1998) (Dot brown line is the basin boundary, basement toward East)

Magnetic Data

The magnetic data of the area were downloaded from the MagBrasil project (CPRM), compiled and homogenized in a grid of 1 km, the total field anomaly in nT. (figure 7), with extension of 200 (EW)by 150 km (NS). Anisotropy is notable associated with lithologic domains and faults.

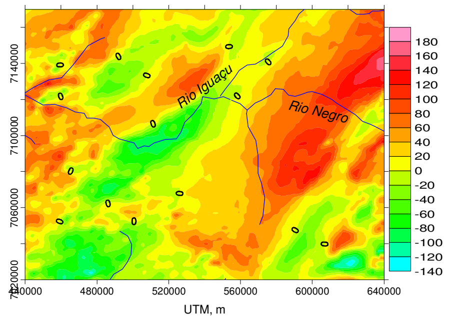

Figure 7 - Contoured anomalous magnetic field values (nT) of worked area (data compiled and homogenized by CPRM)

Operating procedures

The area was divided into 4 sub-areas of 60kmx60km, with overlay. The grid base was 1 km, with search window for calculation of variogram and covariogram extending up to 90 km. Preliminary variographic analysis has showed the high anisotropy toward N40E-S40W. The variogram pairs were obtained in that direction, with angular tolerance of 15 degrees and linear equal to half size of the lag to remove the cumulative effect of the variability in distance smaller than the half wavelength of the lag size.
Along the variogram, a three point moving average of γ(x) was considered in order to choose automatically the closer and longest point with positive 1^{st} derivative and null 2^{nd} derivative were. These points (pxi), were selected and the values of the corresponding covariance captured as the power of the waves of length 1 and 2: Cv1(px1) and Cv2 (px2) equivalent to *F(λ1)* and *F(λ2)*. With these values *zt* and *zb* were calculated . The procedures were performed automatically on specific software (GAM_DPC, in consolidation)..

Results and discussion

The results of the calculations for a 10km squared grid and saved in two spreadsheets. The first save cell number, XY coordinates, averaged *γ(x,y) and Cv(x,y), zt, zb.* Rejected cell for inconsistency are masked.
Te map was made by minimum curvature interpolation and contouring of depth of the Curie surface and presented in Figure 8.
The results and the map show consistency with the values expected based on the determination of PC by heat flow, The range is the same from 80 to 15 mW/m^2, respectively in green-blue color and red-purple boundaries, as may be compared with figure 6. Anomalous values in ground heat flow have correspondence to the estimated by the method. Known fault zones extensions from Pien (FP), Lancinha (FL) and Itapirapuã (FI) as lineaments are well delineated by anomalies of shallow Curie surface.

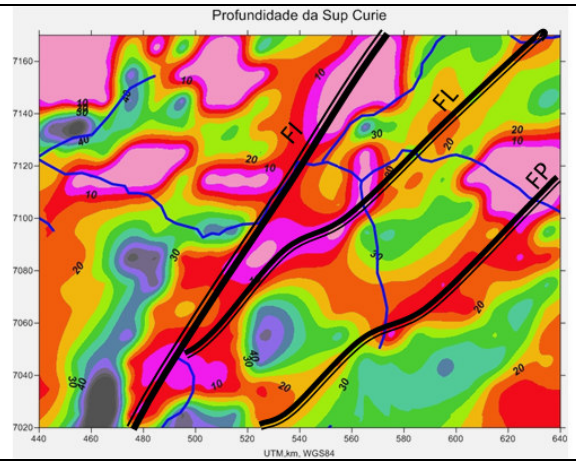

Figure Results for depth of Curie surface in worked area (X 440-640 km, Y 7020-7170 km. Failures Itapirapuã (NNE) and Lancinha (FL) and Pien (FP) contour = 5 km; range 5 to 80 km. Red, 10 to 20 km.

Conclusions

The use of anisotropic variograms and covariograms functions the Curie surface depths. Were estimated over an structurally complex area in eastern part of Parana basin. Anomalies of shallow Curie surface around 15 km depth, occur in narrow NE-SW zones and are closely associated with fault extension from basement and lineaments, as Pien, Lancinha and Itapirapuã faults. The shallow zones coincides with local anomalous high values of heat flow, as M. Mallet.

Regionalized anisotropic analysis of variance constitutes an appropriate methodological set to estimate the depth of Curie surface from magnetic data. Among the benefits are the fact that the variance is estimated from a vector floating over the set of data, taking into account the distance and direction. This enables high flexibility in terms of window and tolerance, and formulation of algebraic estimation as a function of wavelength.

References

AYDIN, I. AND OKSUM , E., 2010. Exponential approach to estimate the Curie-temperature depth. IOP PUBLISHING. **J. Geophys. Eng**. **7** (2010) 113–125 doi:10.1088/1742-2132/7/2/001

BHATTACHARYYA B K 1966. Continuous spectrum of the total-field magnetic anomaly due to rectangular prismatic body. ***Geophysics* 31** 97–121

BLAKELY, 1995. BLAKELY R J 1988 Curie temperature isotherm analysis and tectonic implications of the aeromagnetic data from Nevada ***J. Geophys.*** *Res.* **93** 11817–32;

BLUM, M.L.B. & PIRES, A.C.B. 1996. Superfície Curie da região central de Goiás. **Rev. Bras. Geoc**., **26**(3):197-208.

BLUM, M.L.B. 1999. Processamento E Interpretação de Dados de Geofísica Aérea No Brasil Central E sua Aplicação a Geologia Regional E À Prospecção Mineral. Inst. Geoc, Unb, Brasília, Tese Doto, 229p.

FERREIRA, F. J. F. ; BLUM, M. L. B. ; FORLIN, M. ; SOARES, P. C. ; ROSTIROLLA, S. P. Superfície Curie da Região de Fartura, SP-PR. In: XXXIX **Anais Cong. Bras. Geol**., 1996,. Salvador-Ba:SBG-BA/SE, 1996. v. II. p. 338-340.

HURTER S. J.& POLLACK 1996. Terrestrial heat flow in the Parana Basin, Southern Brazil. **J. Geoph Res**, v. 101, B4, 8659-8671.

MADEN, N. 2009. Curie-point Depth from Spectral Analysis of Magnetic Data in Erciyes Stratovolcano (Central TURKEY). **Pure Appl. Geophys.** 167 (2010), 349–358

MAUS, S., D. GORDON & D.FAIRHEAD (1997). Curie-temperature depth estimation using self similar magnetization model. **Geophys. J. Int 129**:163-168)

HAMZA V.M. & MUNHOZ, M. 1996. Heat flow map of South America. **Geothermics**, 25(6):599-646

NAIDU, P. 1968. Spectrum of the potencial field due to randomly distributed sources. **Geophisics 33**, 337-345.

OKUBO, Y. GRAF, R.J., HANSEN, R.O., OGAWA, K & TSU, H, 1985 – Curie point depths fo the island of Kyushu and surrounding areas, Japan. Geophysics, 53:481-494. 4º. **Cong. Intern. Soc. Bras. Geof**., v. 1:240-242.

SOARES, ANA PAULA ; SOARES, PAULO CESAR ; BETTU, D.F. ; Holz, Michael . Compartimentaçao estrutural da Bacia do Paraná: a questão dos lineamentos e sua influência na distribuição do Sistema Aquífero Guarani. **Geociências (SAo Paulo),** v. 26, p. 297-311, 2007

SOARES, P. C., ROSTIROLLA, S. P., FERREIRA, F. J. F. & STEVANATO, R., 1996. The Pitanga-Quatigua-Jacutinga structural high in the Paraná Basin: a lithospheric structure. Thematic Symp.Tectonics Sedimentn in South American Basins, **SAMC News 5**, Ext Abst, pp. 80-82

ROCHA, P. L.F. 1998. Estudo da litosfera do Brasil entre os paralelos de 17S e 33S a partir de dados gravimétricos, magnéticos e de fluxo de calor. Pub. Esp.07/98. SNPq/ON.Rio de Janeiro,159 p.

TANAKA, A., Okubo, Y., and MATSUBAYASHI, O. (1999), Curie-point depth based on spectrum analysis of the magnetic anomaly data in East and Southeast Asia, **Tectonophysics** 306, 461–470.